

Picturing perturbative parton cascades in QCD matter

Aleksi Kurkela and Urs Achim Wiedemann¹

¹Physics Department, Theory Unit, CERN, CH-1211 Genève 23, Switzerland

Based on parametric reasoning, we provide a simple dynamical picture of how a perturbative parton cascade, in interaction with a QCD medium, fills phase space as a function of time.

I. INTRODUCTION

There are essentially two motivations for studying how a perturbative parton shower, embedded in QCD matter, evolves on all energy scales and on all angular scales. First, this process has been recognized since long as a useful set-up for elaborating the dynamics of thermalization in QCD [1]. This is so, since the parton distribution characterizing a jet is initially far from equilibrium, but in a thermal QCD medium it will evolve at late times into a distribution that is indistinguishable from a thermal one. In this context, recent detailed analyses have determined for instance that the thermalization time obtained from a weak coupling treatment [2–4] is comparable to that established for non-abelian gauge theories in the strong coupling limit [5–8]. Secondly, studying the medium-modifications of perturbative parton showers is motivated, of course, by the recent measurements of reconstructed jets in heavy ion collisions at the LHC [9–16] that characterize in unprecedented detail the medium-induced redistribution of jet energy and jet quanta in longitudinal (*i.e.* along the jet axis) and transverse (*i.e.* orthogonal to the jet axis) phase space. While it is conceivable that strong coupling techniques are needed to explain these data [17], the observation of modified but vacuum-like fragmentation patterns [11, 12] in high energy jets at the LHC gives support to approaches that formulate medium effects within a perturbative framework [18]. Recent approaches extend the early perturbative formulation of medium-induced parton energy loss [19–25] in particular by better analyzing the role of color coherence and transverse broadening in the evolution of the medium-modified perturbative parton cascade [26–34], and by developing full Monte Carlo models for medium-modified parton showers [35–37].

Remarkably, the recent developments towards a jet quenching phenomenology applicable to all jet energy and angular scales, as well as the recent studies of the conceptually related thermalization problem, have identified largely independent of each other a set of parametric momentum scales and angular scales that characterize different aspects of the jet quenching phenomenon. The present work grew out of our attempt to combine, what is parametrically known from these studies, into a simple dynamical picture of how a perturbative parton cascade embedded in thermal QCD matter fills phase space as a function of time. In elaborating this picture, we came across parametric estimates of physics effects that we had not seen discussed before, such as parametric estimates for the interplay between vacuum and medium-induced

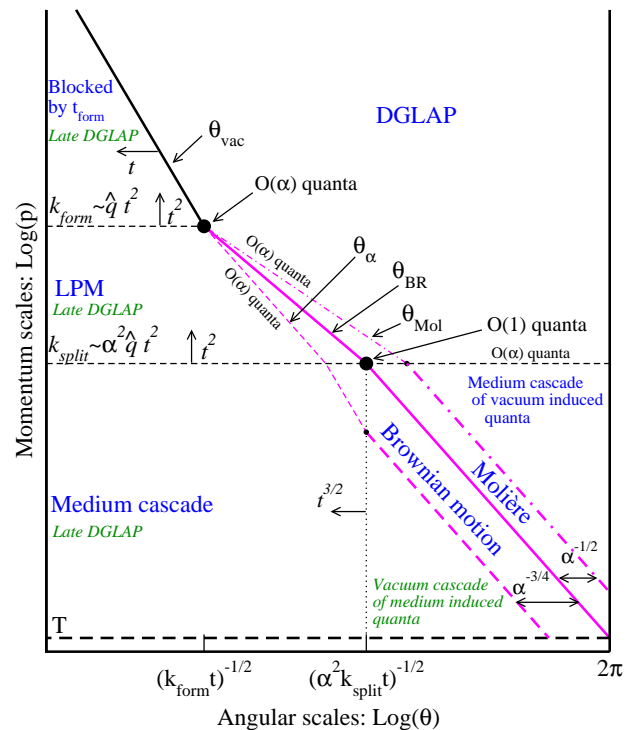


FIG. 1: Parametrically accurate picture of how a medium-modified parton cascade fills phase space. At time t , quanta can be formed up to momentum scale k_{form} and they are formed with $O(1)$ probability per $\log p$ at lower scale k_{split} . Quanta below k_{split} split further and their energy cascades to the thermal scale T in less than an epoch t . Transverse Brownian motion moves quanta up to the angle $\theta_{\text{BR}}(p)$ denoted by the thick purple line. The Molière region at larger θ is dominated by rare large angle scattering. At even larger angle, there are $O(\alpha_s)$ quanta per double logarithmic phase space from DGLAP ‘vacuum’ radiation, and for momenta below k_{split} these cascade within time t to T . After the jet escapes the medium, the jet and the emitted fragments will undergo vacuum radiation. This late time vacuum radiation emitted by the original parton dominates at sufficiently small $\log \theta$ (regions marked “late DGLAP” and bounded by θ_{vac} and θ_α), whereas the late time radiation of the fragments dominates in the region denoted by “Vacuum cascade of the medium induced quanta”. Details given in the text.

radiation, for the medium-induced cascading of DGLAP vacuum radiation to lower momentum scales, for the late time (*i.e.* after the jet has left the medium) vacuum cascading of medium-induced radiation, and for the angular scales at which rare large angle scattering dominates over

multiple soft angle scattering. Including these effects, we provide in section II a simple, kinematically complete and parametrically correct picture of the evolution of a perturbative parton cascade in QCD matter. We then illustrate the use of this picture by relating parametric estimates of the jet energy fraction of different kinematical regions to characteristic features in the measurements of quenched jets.

II. JET EVOLUTION IN THE $\log p$ - $\log \theta$ -PLANE

In this section, we motivate Fig. 1 that illustrates what happens parametrically in perturbation theory when a jet propagates through a thermal cloud of temperature T . We consider a set up in which, at very early time $t = 1/Q \sim 0$, a hard parton distribution $\sim \delta(\theta) \delta(p - Q)$ is embedded in the thermal bath. This ‘jet’ is localized in angle θ , and it lives at time $t = 0$ on a momentum scale Q that is much larger than any other scale in the problem. Subsequently, the jet evolves via perturbative parton branching. Fig. 1 depicts how its fragments (‘splittees’) fill the logarithmic phase space in momentum p and angle θ as a function of time. We aim at a discussion that is based on minimal assumptions about the nature of the QCD matter. For simplicity, the medium is assumed to be time-independent, and - for most of our arguments - it is assumed to be characterized solely by the transport coefficient \hat{q} that denotes the medium-induced squared transverse momentum broadening of energetic partons per unit path-length. Whenever our estimates rely on more detailed information about the microscopic structure of the QCD medium, we shall state this explicitly.

A. DGLAP region

Quantum mechanical formation time prevents emission faster than a time it takes to separate the wave packets of the splitter and the splittee. In general, splittees at a scale $p < Q$ can form at a time $t \geq p/k_{\perp}^2$ set by their inverse transverse energy. For jet evolution in the vacuum, the angular distribution is determined by the primary decay kinematics of the splittee, $t \geq p/k_{\perp}^2 \sim 1/(p\theta^2)$. Therefore, the logarithmically ordered DGLAP (Dokshitzer-Gribov-Lipatov-Altarelli-Parisi) ‘vacuum’ parton shower fills the $\log p$ - $\log \theta$ -plane from the outside in. In the entire region determined by $\theta > \theta_{\text{vac}}$ with

$$\theta_{\text{vac}} \sim 1/(pt)^{1/2}, \quad (1)$$

one finds with a probability $O(\alpha_s)$ per logarithmic phase space quanta due to vacuum radiation,

$$\frac{dP_{\text{find}}}{d \log p d \log \theta} \sim \alpha_s. \quad (2)$$

The region where this primary splitting gives the dominant contribution in the $\log p$ - $\log \theta$ -plane is marked as the DGLAP-region in Fig. 1.

B. LPM region

In contrast, medium-induced parton branching fills the $\log p$ - $\log \theta$ -plane from the bottom up (in p) and from the inside out (in θ) [19]. This is so since transverse momentum is acquired by Brownian motion in the medium, $k_{\perp}^2 \sim \hat{q} t$; the formation time constraint $t \geq p/k_{\perp}^2 \sim p/(\hat{q} t)$ implies then that medium-induced quanta can be formed in the region $p \lesssim k_{\text{form}}$ where

$$k_{\text{form}}(t) \equiv \hat{q} t^2, \quad (3)$$

or, alternatively, that quanta at a scale p can be formed at times $t > t_{\text{form}}(p)$ where

$$t_{\text{form}}(p) \equiv \sqrt{\frac{p}{\hat{q}}}. \quad (4)$$

These quanta are created at small angles $\theta \lesssim \sqrt{\alpha_s}$, and to our purposes we can treat the emitted quanta as being collinear with respect to the emitter.¹ Their angular distribution will be determined by reinteractions with the medium, discussed in section II F.

A quantum can be formed at the scale k_{form} , but in a weakly coupled theory, it is formed only with a probability α_s . Therefore, at the scale k_{form} , there are $O(\alpha_s)$ quanta per logarithmic phase space due to medium-induced parton branching. At scales below k_{form} (denoted as the LPM-region in Fig. 1) the formation time is faster $t_{\text{form}} < t$, and as a result of this the medium-induced splittings become more and more abundant as one moves from the scale k_{form} to an increasingly softer scale $p < k_{\text{form}}$. There is an $O(\alpha_s)$ probability of emitting a splittee at the scale p at every $t_{\text{form}}(p)$ and thus the probability of finding a splittee with a momentum p with $p < k_{\text{form}}$ is parametrically²

$$\frac{dP_{\text{find}}(t)}{d \log p} \sim \alpha_s t / t_{\text{form}}(p) \sim \alpha_s \hat{q}^{1/2} p^{-1/2} t. \quad (6)$$

While $t_{\text{form}}(p)$ determines the minimal duration for a quantum to be created with probability $O(\alpha_s)$, the parametrically longer time

$$t_{\text{split}}(p) \sim t_{\text{form}}(p) / \alpha_s \quad (7)$$

¹ The angle at which a quantum is created is $\theta^2 \sim \hat{q} t_{\text{form}} / p^2$, which for a perturbative medium $\hat{q} \sim \alpha_s^2 T^3$ reads $\theta^2 \sim \alpha_s (T/p)^{3/2}$.

² At leading order, for $p \ll Q$, the prefactor can be extracted, *e.g.*, from the splitting function of [1, 38], and in numerical form the spectrum reads

$$\frac{dP_{\text{find}}(t)}{d \log p} \approx \frac{1}{\pi} C_A \alpha_s p^{-1/2} \hat{q}^{1/2} (p) t. \quad (5)$$

is needed to create this quantum with probability ~ 1 . At fixed time t , the quanta that are created thus with $O(1)$ probability live at the scale $p \sim k_{\text{split}}$

$$k_{\text{split}}(t) \sim \alpha_s^2 k_{\text{form}}(t) \sim \alpha_s^2 \hat{q} t^2, \quad (8)$$

which marks the end of the LPM-region in Fig. 1.

C. Medium Cascade

Not all quanta that are created will stay where they were created. Those modes that have time to lose a significant fraction of their energy will cascade to a significantly lower scale p . For LPM-type radiation, the splitting that degrades energy the most is the hardest splitting and the hardest splitting available is the quasi-democratic one.³

The timescale for a quasi-democratic splitting is of the same order of magnitude as the splitting time $t_{\text{split}}(p)$ at the same scale. This is so because, in a non-abelian theory, the parametric emission time for LPM-type radiation is independent of the momentum of the parent and is set by the momentum of the softer splittee, which for a quasi-democratic splittings is parametrically of the same order as the parent momentum.

A quasi-democratic splitting moves the energy deposited at scale p to a lower scale of $p/2$. Parametrically the lower scale, $p/2$, is of the same order as the original p , and therefore even a democratic splitting is a local process in the logarithmic p -space. However, if a given mode has had time to undergo a quasi-democratic splitting, then a successive quasi-democratic splitting of its daughters will take place on a shorter time scale. Therefore, the scales which have had time to undergo a quasi-democratic splitting with $O(1)$ probability can cascade all the way to the scale T of the thermal bath within the same epoch t within which the first democratic splitting occurred [31] (in the context of thermalization, the analogous process was discussed in [1–3]).

To quantify these considerations, we introduce the time $t_{\text{res}}(p)$ that a quantum resides at scale p before splitting further. For $p > k_{\text{split}}$, this residence time must equal the lifetime t of the system, and for lower scales p it must scale like the formation time. We therefore have

$$t_{\text{res}}(p) \sim \begin{cases} t, & \text{for } k_{\text{form}} > p > k_{\text{split}}, \\ \sqrt{\frac{p}{k_{\text{split}}}} t, & \text{for } p < k_{\text{split}}. \end{cases} \quad (9)$$

The energy ϵ in this cascade is dominated by the hardest scale that can cascade, $\epsilon = n(k_{\text{split}})k_{\text{split}} \approx k_{\text{split}}$. This energy will move through all scales p down to T via quasi-democratic splittings, and since quanta spend

a shorter time $t_{\text{res}}(p)$ at lower momentum scale, only the fraction $t_{\text{res}}(p)/t$ of quanta that arrived within the residence time will not have left already and will therefore contribute to the energy at the scale $p < k_{\text{split}}(p)$,

$$\frac{d\epsilon}{d \log p} = p \frac{dn}{d \log p} \sim k_{\text{split}} \frac{t_{\text{res}}(p)}{t} \sim \alpha_s \sqrt{\hat{q} p t}. \quad (10)$$

By coincidence, the energy distribution (10) in the region of the medium cascade matches the distribution in the LPM region since $k_{\text{split}} \frac{t_{\text{res}}(p)}{t} \sim p t / t_{\text{split}}(p)$. Accordingly, also the number of quanta per $\log p$ shows the same $1/\sqrt{p}$ -dependence as in the LPM region,

$$\frac{dn}{d \log p} = \frac{1}{p} \frac{d\epsilon}{d \log p} \sim \alpha_s \sqrt{\hat{q} t} / \sqrt{p}. \quad (11)$$

This similarity is particular to the \sqrt{p} power law. We emphasize that despite these similarities, the physics in the region of the medium cascade and in the LPM region are somewhat different.

D. Medium cascade of the vacuum quanta

The quanta produced in the DGLAP region will also undergo medium interactions that will make the quanta radiate and split. The distribution of radiation from the vacuum quanta is the same as from any other mode. Therefore the distribution of the daughters originating from the medium quanta above k_{split} is

$$\frac{dP_{\text{find}}}{d \log p d \log \theta} \sim \alpha_s \frac{t}{t_{\text{split}}(p)}, \quad (12)$$

where α_s is just the number of vacuum quanta per double logarithmic unit of phase space. Again, the ratio $t/t_{\text{split}}(p)$ is smaller than 1 for modes above k_{split} , and therefore the number of daughters is smaller than the number of vacuum splitted quanta.

Below k_{split} , however, both $t/t_{\text{split}}(p) > 1$ and $t/t_{\text{res}}(p) > 1$, leading to a cascade that is similar to the medium cascade discussed above. With the same arguments the number of quanta becomes

$$\frac{dn}{d \log p d \log \theta} \sim \alpha_s \frac{t}{t_{\text{split}}(p)} \quad \text{for } p < k_{\text{split}}(p). \quad (13)$$

E. Absence of Bethe-Heitler region

We have argued that from k_{form} down to the momentum scale p , particle radiation is LPM suppressed. Given that formation times decrease with decreasing p , one may wonder why there is not a softer momentum scale at which individual quanta in the heat bath are resolved and an un-suppressed Bethe-Heitler radiation pattern $n(p) \propto 1/p$ off independent scattering centers results. To discuss this possibility, we need to introduce

³ Splittings where both splittees carry $O(1)$ of the parent momentum will be referred to as 'quasi-democratic' in the following.

microscopic characteristics of the perturbative medium that we have in mind. The small angle scattering time in this medium will be $\tau_{\text{scatt}} \sim 1/(\alpha_s T)$, and $\hat{q} \sim \alpha_s^2 T^3$ [39–41]. The cross-over to a Bethe-Heitler region is then expected to take place at the scale k_{BH} determined by

$$t_{\text{form}}(k_{\text{BH}}) \sim \tau_{\text{scatt}}, \quad (14)$$

which implies

$$k_{\text{BH}} \sim T. \quad (15)$$

Therefore, only the infrared tail of the medium cascade has an $O(1)$ Bethe-Heitler correction whereas the LPM-suppressed splitting gives a good description of the radiation at all higher scales $p > k_{\text{BH}} \sim T$.

F. Angular distribution

We discuss now the angular distribution of quanta on the different momentum scales p . There are two mechanisms. First, multiple soft scattering gives rise to transverse Brownian motion and determines the distribution at small angles. Second, rare large angle scattering leads to deviations from Brownian motion that were first described by Molière for QED [42]. This Molière scattering will put quanta at large angular scales that cannot be reached by Brownian motion in time t .

1. Angular distribution at small θ

In general, transverse Brownian motion moves quanta by an angle

$$\theta_{\text{BR}}^2 \sim \frac{k_{\perp}^2}{p^2} \sim \frac{\hat{q} t_{\text{res}}(p)}{p^2}, \quad (16)$$

that is set by the time $t_{\text{res}}(p)$ that the quantum resides and thus broadens at scale p . Quanta with $p > k_{\text{split}}$ will have spent a time of order of the duration of the jet evolution at p , that means, $t_{\text{res}}(p) \sim t$. Therefore, these quanta reach a typical angle

$$\theta_{\text{BR}}(p) \sim \frac{\sqrt{\hat{q}t}}{p} \quad \text{for } k_{\text{form}} > p > k_{\text{split}}. \quad (17)$$

This is the limiting angle up to which the LPM region extends in Fig. 1. This angle reaches from

$$\theta_{\text{BR}}(k_{\text{form}}) \sim \frac{1}{\sqrt{k_{\text{form}} t}} \quad (18)$$

at the upper bound of the LPM region to a parametrically larger angle

$$\theta_{\text{BR}}(k_{\text{split}}) \sim \frac{1}{\sqrt{\alpha_s^2 k_{\text{split}} t}} \sim \frac{1}{\alpha_s^2 \sqrt{k_{\text{form}} t}} \quad (19)$$

at the lower bound. For $p < k_{\text{split}}$, where resplitting happens, the time $t_{\text{res}}(p)$ a quantum stays at the scale p before leaving by undergoing a quasi-democratic splitting is shorter than the lifetime of the system, $t_{\text{res}}(p) < t$, and this shortens the typical angle reached by transverse Brownian motion in the region of the medium cascade,

$$\theta_{\text{BR}}^2(p) \sim \frac{\hat{q} t_{\text{res}}(p)}{p^2} \sim \frac{\hat{q} t}{p^{3/2} k_{\text{split}}^{1/2}} \quad \text{for } p < k_{\text{split}}. \quad (20)$$

It is remarkable that in the region of the medium cascade this angle does not change with evolution time t , although many other scales in Fig. 1 do. In fact, if one adopts the perturbative estimate $\hat{q} \sim \alpha_s^2 T^3$, one finds that this angle is set by the simple ratio of momentum scales,

$$\theta_{\text{BR}}(p) \sim \left(\frac{T}{p}\right)^{3/4}. \quad (21)$$

This way of rewriting equation (20) makes it also clear that $p \sim T$ is the largest scale that isotropizes.

Since Brownian motion leads to a Gaussian distribution in $d^2\theta$, which is parametrically flat for $\theta < \theta_{\text{BR}}$, the energy contained in this region in a double logarithmic unit of phase space is

$$\frac{d\epsilon}{d \log p d \log \theta} \sim p \frac{t}{t_{\text{split}}(p)} \frac{\theta^2}{\theta_{\text{BR}}^2}. \quad (22)$$

Before concluding this subsection, we point out as an aside that there is a logarithmic enhancement at small θ . The reason is that the particles created later have had a shorter time to broaden and this effect accumulates quanta in the collinear region. To be specific, consider the contribution of some last small time interval $\alpha_s^b t$ to the radiation. It is

$$\frac{dP_{\text{create}}}{d \log(p)} \sim \alpha_s^b \frac{t}{t_{\text{split}}(p)} \quad (23)$$

and these radiated quanta appear under the angle

$$\theta_b^2 \sim \hat{q} \alpha_s^b t / p^2. \quad (24)$$

Therefore in the differential probability distribution, the α_s^b 's cancel, and all logarithmic times make an equally large contribution to all logarithmic bins they can reach. Therefore, one expects to see a logarithmic enhancement of equation (22) in the collinear region.

2. Angular distribution in the Molière scattering region

So far, our estimates did not rely on assumptions about the microscopic structure of the medium. If hard scatterings resolve partonic constituents in the medium, then these rare occurrences can move a quanta to angles $\theta > \theta_{\text{BR}}$ [43]. At scale $p \in [T, k_{\text{form}}]$, there are $t/t_{\text{split}}(p)$

quanta per $\log p$ and each of them will undergo a hard momentum transfer $q_{\perp} = p\theta$ during their stay at the momentum scale p with probability [39–41]

$$\frac{dP_{\text{kick}}}{d\log\theta} \sim \alpha_s^2 \frac{n_T}{p^2 \theta^2} t_{\text{res}}(p) \quad (25)$$

where $n_T \sim T^3$ is the number density of resolvable scattering centers. Multiplying these numbers, we get the probability to find a quantum at large angles⁴

$$\frac{dP_{\text{find}}}{d\log p d\log\theta} \sim \begin{cases} \alpha_s^3 n_T t^2 \hat{q}^{1/2} / (p^{5/4} \theta)^2 & \text{for } p > k_{\text{split}} \\ \alpha_s^2 n_T t / (p\theta)^2 & \text{for } p < k_{\text{split}}. \end{cases} \quad (26)$$

We find that along lines $p \propto \theta^{-4/5}$ for $p > k_{\text{split}}$ (or $p \propto \theta^{-1}$ for $p < k_{\text{split}}$), there is a fixed number of quanta per double logarithmic phase space. Since this is a power-law dependence in θ while Brownian motion dies out exponentially above θ_{BR} , rare hard Molière scattering, if allowed for by the microscopic structure of the medium, will dominate the distribution of medium-induced quanta above θ_{BR} .

Comparing the probability distribution (26) for Molière scattered quanta at large angle $\theta > \theta_{\text{BR}}(p)$ to that of vacuum quanta (eq. (2) for $p > k_{\text{split}}$) and to that of vacuum quanta undergoing the medium cascade (eq. (12) for $p < k_{\text{split}}$), we find that outside a relatively narrow region of logarithmic phase space, the DGLAP vacuum radiation (thin dash-dotted line in Fig. 1), or the cascade of the vacuum quanta (thick dash-dotted line in Fig. 1), will overshadow the contribution from Molière scattering. The quanta sensitive to the microscopic structure give a dominant contribution to the energy only for $\theta < \theta_{\text{Mol}}$ with

$$\theta_{\text{Mol}} \sim \begin{cases} \alpha_s t n_T^{1/2} \hat{q}^{1/4} p^{-5/4} & \text{for } p > k_{\text{split}} \\ n_T^{1/2} \hat{q}^{-1/4} p^{-3/4} & \text{for } p < k_{\text{split}}. \end{cases} \quad (27)$$

Here, the expression for $p < k_{\text{split}}$ can be written in a form resembling equation (21)

$$\theta_{\text{Mol}} \sim \frac{1}{\alpha_s^{1/2}} \left(\frac{T}{p} \right)^{3/4} \quad \text{for } p < k_{\text{split}}, \quad (28)$$

As already observed for θ_{BR} , also the angular limit θ_{Mol} for Molière scattering is independent of time within the region of the medium cascade.

G. Extending Fig. 1 to $t > t_{\text{form}}(Q)$

So far in our consideration, we have made the assumption that Q is the hardest scale in the system. The scales

k_{form} and k_{split} , however, grow fast $\propto t^2$, and eventually they will reach the scale Q . In the following we discuss how the dynamics changes after k_{form} and k_{split} reach Q .

When $k_{\text{form}} \sim Q$ (or equivalently $t > t_{\text{form}}(Q)$) the quasi-democratic splitting of the original jet becomes allowed, but it happens only with probability α_s ; successive quasi-democratic splittings are also suppressed by further powers of α_s . Therefore, for a typical jet, no qualitative change happens at $t_{\text{form}}(Q)$. What changes, however, is the average rate at which the leading parton is losing energy $d\langle\epsilon_Q\rangle/dt$; here the brackets are to be understood as an average over an ensemble of independent jets. The energy lost by the leading parton is dominated by the hardest splitting possible, which before $t_{\text{form}}(Q)$ is k_{form} but stays at Q after $t_{\text{form}}(Q)$. The average rate for losing energy depends on the probability of the hardest emission t/t_{split} , and it depends on the energy lost in the event of a hard emission taking place. For $t < t_{\text{form}}(Q)$ the average rate reads [19]

$$d\langle\epsilon_Q\rangle/dt \sim (t/t_{\text{split}}(k_{\text{form}}))k_{\text{form}}/t \sim \alpha_s \hat{q}t, \quad (29)$$

whereas the rate saturates for $t > t_{\text{form}}(Q)$

$$d\langle\epsilon_Q\rangle/dt \sim Qt/t_{\text{split}}(Q) \sim \alpha_s Q^{1/2} \hat{q}^{1/2}. \quad (30)$$

When $k_{\text{split}} \sim Q$ — corresponding to the jet stopping time of $t_{\text{split}}(Q) \sim (Q/T)^{1/2}/\alpha_s^2 T$ [19, 25] — the probability for a democratic splitting of the jet becomes $O(1)$, and the successive democratic splittings will happen in a time scale faster than the time it took for the original splitting. As argued, *e.g.*, in Refs. [1–4, 25, 31], the jet will therefore become quenched and lose all of its energy to the thermal bath in a timescale it takes to undergo the first quasi-democratic splitting.

III. JET QUENCHING IN A FINITE MEDIUM

The picture Fig. 1 discussed in section II is a snapshot at fixed evolution time of the logarithmic phase space distribution of partonic fragments. Some of the phase space boundaries will evolve in time as indicated in the figure, while others will stay put. Therefore, this picture informs us also about how the jet quenching process occurs dynamically as a function of time.

In the phenomenologically realized situation, the jet propagates over a finite path-length L in QCD matter, and (for sufficiently short $L < t_{\text{form}}(Q)$, see details below) Fig. 1 thus represents the distribution of partonic jet fragments at moment $t \sim L$ when the jet escapes the medium. In the following, we discuss in more detail the energy distribution of the quenched parton shower at that moment, and the physics that modifies this distribution at later times and for longer path lengths.

⁴ Another possibility to create a quantum at large angles would be directly through a hard scattering. The probability for this would then be $P_{\text{find}} \sim \alpha_s \times P_{\text{kick}}$. However, whenever a quantum can be formed, $t/t_{\text{split}} > \alpha_s$, and this process gives only a subleading correction.

A. Vacuum radiation for $t > L$

The typical virtuality of quanta at time $t \sim L$ is $O(\hat{q} t_{\text{res}}(p))$. The dominant mechanism that further degrades this virtuality in the subsequent vacuum evolution is soft and collinear splitting. On the one hand, this mechanism does not move appreciably the emitter in $\log \theta$ and $\log p$, on the other hand, it puts $O(\alpha_s)$ quanta in the double logarithmic phase space below any emitter. Therefore, late time fragmentation affects the distributions of Fig. 1 only in those regions of phase space in which there are less quanta than $O(\alpha_s)$ times the number of quanta at higher momentum scales in the corresponding angular scale at time $t \sim L$. As we explain now, this is only the case in the collinear region of sufficiently small $\log \theta$, where momentum broadening and smallness of angular phase space have resulted in a small density of medium-induced quanta, and in a sufficiently soft region at large angle where there are sufficiently many medium-induced quanta at higher momentum scale that can split further at late times.

1. Radiation of vacuum quanta at $t > L$

At small angular scales $\theta < \theta_{\text{BR}}(k_{\text{split}}) \sim (\alpha_s^2 k_{\text{split}} t)^{-1/2}$, there are less than 1 medium induced quanta integrated over p and therefore late vacuum fragmentation is dominated by the original single parton at the scale Q . This becomes dominant over the medium-induced distribution when there are less than $O(\alpha_s)$ medium induced quanta per double logarithmic unit of phase space. This small-angle region $\theta(p) < \theta_\alpha(p)$, in which vacuum radiation dominates is obtained by requiring that (22) is larger than $\alpha_s p$,

$$\theta_\alpha(p) \sim \sqrt{\alpha_s} \theta_{\text{BR}}(p) \sqrt{\frac{t_{\text{split}}(p)}{t}}. \quad (31)$$

This region is delineated by the thin dashed line between k_{split} and k_{form} in Fig. 1. We note that the contribution of this late time vacuum splitting to jet observables will be that of a vacuum jet, but one of degraded energy. For an ensemble average, the reduced energy of this vacuum jet contribution is given by equations (29) and (30),

$$\langle Q' \rangle = Q - \langle \epsilon_Q \rangle \sim Q - \begin{cases} \alpha_s k_{\text{form}} & \text{for } t < t_{\text{form}}(Q) \\ \alpha_s Q^{1/2} \hat{q}^{1/2} & \text{for } t > t_{\text{form}}(Q). \end{cases} \quad (32)$$

In principle, late time splitting of vacuum quanta contributes also to $\theta > \theta_{\text{BR}}(k_{\text{split}})$. In this region of the medium-cascade, however, there is also a contribution from the late time vacuum splitting of medium-induced quanta to which we shall turn next. Since this latter contribution dominates, we do not continue in Fig. 1 the line of $\theta_\alpha(p)$ into the region $\theta > \theta_{\text{BR}}(k_{\text{split}})$ corresponding to $p < k_{\text{split}}$.

2. Radiation of medium-induced quanta at $t > L$

Most of the medium-induced quanta reside on the angular scale $\theta_{\text{BR}}(p)$. Correspondingly, for a given angular scale $\theta > \theta_{\text{BR}}(k_{\text{split}})$, the number of medium-induced quanta is dominated by the momentum scale

$$p_{\text{BR}}(\theta) \sim \left(\frac{\theta_{\text{BR}}}{\theta} \right)^{4/3} p. \quad (33)$$

For these angular scales, the number of the medium-induced quanta along $\theta_{\text{BR}}(p)$ exceeds $O(1)$ per double logarithmic phase space. Therefore, the late time vacuum splitting of these more than $O(1)$ medium-induced quanta dominates over the vacuum splitting of the $O(1)$ vacuum quantum described in section III A 1 above.

For a fixed θ , the number of quanta at the scale p_{BR} reads

$$\frac{dn}{d \log p d \log \theta} \sim \frac{t}{t_{\text{split}}(p)} \frac{t_{\text{split}}(p)}{t_{\text{split}}(p_{\text{BR}})} \sim \frac{t}{t_{\text{split}}(p)} \left(\frac{\theta}{\theta_{\text{BR}}} \right)^{2/3}. \quad (34)$$

Then the number of emitted quanta by the medium induced fragments at the scale p_{BR} to all scales below is

$$\frac{dn_{\text{late vac}}}{d \log p d \log \theta} \sim \alpha_s \frac{t}{t_{\text{split}}(p)} \left(\frac{\theta}{\theta_{\text{BR}}} \right)^{2/3}. \quad (35)$$

This dominates over the medium-induced quanta for

$$\theta < \theta_\alpha \sim \alpha_s^{3/4} \theta_{\text{BR}} \quad \text{for } \theta > \theta_{\text{BR}}(k_{\text{split}}). \quad (36)$$

This condition extends the θ_α -line to larger angular scales $\theta_\alpha > \theta_{\text{BR}}(k_{\text{split}})$. We have denoted this extension by a thicker dashed purple line in Fig. 1 to emphasize that there are more than $O(\alpha_s)$ quanta along this line for $\theta_\alpha > \theta_{\text{BR}}(k_{\text{split}})$.

B. Difference in energy degradation of leading hadrons and jets

Since leading hadrons are the leading fragments of leading partons, the total energy $\alpha_s k_{\text{form}}$ radiated away from Q up to time t due to medium effects sets the scale for the suppression of leading hadrons.⁵ In contrast, what is radiated away from the leading parton is not necessarily radiated outside the phase space within which the jet is reconstructed. It is only the energy in scales $p < k_{\text{split}}$ that has had time to undergo the medium cascade and that therefore escapes for sure to sufficiently large angles [1, 2, 31]. The energy missing from the reconstructed jet is thus given by

$$\epsilon_{\text{jet}} \sim k_{\text{split}} \sim \alpha_s^2 \hat{q} t. \quad (37)$$

⁵ As explained in Ref.[44], the typical energy shift seen in leading hadron spectra can be significantly smaller than $\alpha_s k_{\text{form}}$ due to trigger bias effects.

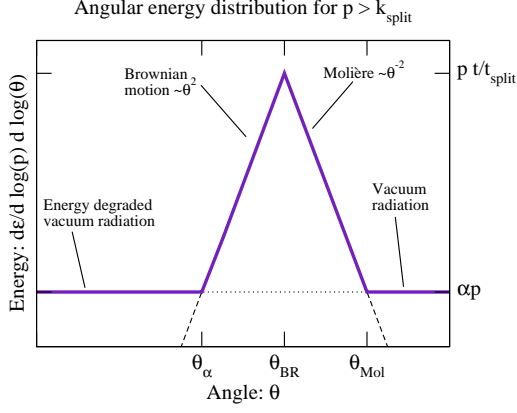


FIG. 2: Double logarithmic sketch of the distribution of energy as a function of angle for a fixed $p > k_{\text{split}}$. The large angular scales $\theta > \theta_{\text{Mol}}$ are dominated by DGLAP vacuum radiation from the leading parton at the scale Q . At small angular scales $\theta < \theta_\alpha$ the energy density is dominated by vacuum radiation of the leading parton after it has degraded its energy propagating through the medium. Medium induced radiation is centered around the angular scale θ_{BR} : for $\theta_\alpha < \theta < \theta_{\text{BR}}$ the angular spectrum is that of Brownian motion whereas for $\theta_{\text{BR}} < \theta < \theta_{\text{Mol}}$ the spectrum arises from Molière scattering. The medium induced contributions (dashed lines) grow as a function of evolution time with respect to the vacuum one (dotted line).

Fig. 1 therefore implies that for all in-medium path lengths $L < t_{\text{split}}(Q)$, $d\langle\epsilon_Q\rangle/dt > d\epsilon_{\text{jet}}/dt$, and thus leading hadrons are more suppressed than reconstructed jets. It is only at the time $t \sim t_{\text{split}}(Q)$ when $k_{\text{split}} = Q$ that $\langle\epsilon_Q\rangle \sim \epsilon_{\text{jet}}$.

C. Angular jet energy distribution

The parametric estimates for the angular distribution of jet energy obtained in this note can be written in a compact form for $p < k_{\text{form}}$

$$\frac{d\epsilon}{d \log p d \log \theta} \sim p \frac{t}{t_{\text{split}}(p)} \times \begin{cases} \alpha_s(t_{\text{split}}(p)/t) & \text{for } \theta < \theta_{\text{BR}}(k_{\text{split}}), \\ \alpha_s(\theta/\theta_{\text{BR}})^{2/3} & \text{for } \theta_{\text{BR}}(k_{\text{split}}) < \theta < \theta_\alpha, \\ (\theta^2/\theta_{\text{BR}}^2) & \text{for } \theta_\alpha < \theta < \theta_{\text{BR}}, \\ (\theta_{\text{BR}}^2/\theta^2) & \text{for } \theta_{\text{BR}} < \theta < \theta_{\text{Mol}}, \\ \alpha_s t_{\text{split}}(p)/t_{\text{res}}(p) & \text{for } \theta > \theta_{\text{Mol}}. \end{cases} \quad (38)$$

The expression (38) is valid for both, the LPM region, $k_{\text{split}} < p < k_{\text{form}}$, and the region of the medium cascade, $p < k_{\text{split}}$. The second of the five conditions listed in (38) is realized only when $\theta_{\text{BR}}(k_{\text{split}}) < \theta_\alpha$, which corresponds to $p < \alpha_s^{3/2} k_{\text{split}}$. For $\theta_\alpha < \theta_{\text{BR}}(k_{\text{split}})$, the region dominated by late energy degraded vacuum radiation (first line in eq.(38)) extends up to θ_α and connects

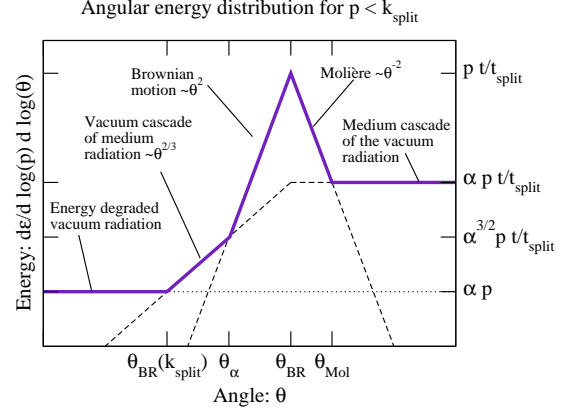


FIG. 3: Double logarithmic sketch of the distribution of energy as a function of angle for a fixed $p < k_{\text{split}}$. At large angles $\theta > \theta_{\text{Mol}}$, in-medium fragmentation of DGLAP radiation dominates the energy density. In close analogy to the situation in the LPM region depicted in Fig. 2, there is a small angle region dominated by (energy degraded) late DGLAP vacuum radiation, and there is the physics of medium-induced Brownian motion and large angle Molière scattering that dominates to the left and to the right of θ_{BR} , respectively. In addition, there is a window $\theta_{\text{BR}}(k_{\text{split}}) < \theta < \theta_\alpha$ in which the late time vacuum DGLAP radiation originating from the medium-induced splitters dominates the spectrum. This window closes for $p > \alpha_s^{3/2} k_{\text{split}}$ as described in the text. The medium induced contributions (dashed lines) grow as a function of evolution time with respect to the vacuum radiation (dotted line).

directly to the region dominated by Brownian motion of medium quanta.

The angular jet energy distribution (38) is depicted in Figs. 2 (for the LPM-region) and 3 (for the medium cascade region). Figs. 2 and 3 illustrate that indeed, late time vacuum radiation of $O(\alpha_s)$ quanta dominates at angles $\theta < \theta_\alpha(p)$. It is only in the range $\theta_\alpha(p) < \theta < \theta_{\text{Mol}}$ that purely medium-induced contributions dominate. In the regions $\theta_{\text{BR}}(k_{\text{split}}) < \theta_\alpha$ and $\theta > \theta_{\text{Mol}}$ the energy is dominated neither by pure vacuum radiation nor by medium-induced radiation, but is a result of an interplay of both types of radiation. While one may naively have thought that the energy from large angle Molière scattering appears at much larger angles than that from small angle Brownian motion, Figs. 2 and 3 demonstrate that the dominant energy from both contributions pile up at the same angular scale θ_{BR} . It is then only the shape of the angular dependence between θ_{BR} and θ_{Mol} that may give access to microscopic details of jet-medium interaction [43].

We further emphasize that θ_{BR} , θ_α , and θ_{Mol} are independent of evolution time below k_{split} , and that a characteristic medium-induced enhancement is seen at this angular scale. This angular scale is set directly by the temperature, while the only medium-dependent informa-

tion entering the size of the peak is \hat{q} . If this structure would be experimentally accessible, it would thus give direct access to the temperature dependence of \hat{q} . More generally, Figs. 2 and 3 illustrate that the energy per unit of double logarithmic phase space will peak for all momentum scales p on the characteristic scale $\theta_{\text{BR}}(p)$ that is a medium-induced scale. This is a robust expectation for perturbative mechanisms of jet quenching. These parametric considerations may provide a motivation to characterize experimental data on the angular jet energy distribution in $\log \theta$ and to search for such an enhancement.

IV. CONCLUSIONS

The main deliverables of this paper are Figs. 1, 2 and 3 which provide a unified view of the physics underlying jet quenching. As discussed, this view is consistent with many results on jet quenching in the (parametrically recent) literature. We note that all the physics phenomena invoked in our discussion are at least in principle imple-

mented in some of the documented jet quenching models. The contribution of our note is not so much to point to novel physics effects, but to provide a map of the phase space regions in which specific known physics is expected to dominate. For instance, the characterization of the angular distribution of jet energy in Figs. 2 and 3 points to the interest in searching in $\log \theta$ plots (within Monte Carlo studies and within data) for characteristic medium-induced enhancements at scale θ_{BR} that may inform us not only about the temperature and small-angle scattering properties (\hat{q}) of the medium, but also (if one can identify the region of Molière scattering) about its quasi-particle content [43]. We hope that in this and in other ways, the simple Figs. 1, 2 and 3 will be of use in the further discussion of jet quenching phenomena.

Acknowledgments

We thank J.P. Blaizot, J. Ghilgieri, E. Iancu, Y. Mehtar-Tani, A.H. Mueller and K. Zapp for discussions at various stages of this work.

-
- [1] R. Baier, A. H. Mueller, D. Schiff and D. T. Son, *Phys. Lett. B* **502** (2001) 51 [hep-ph/0009237].
 - [2] A. Kurkela and G. D. Moore, *JHEP* **1112** (2011) 044 [arXiv:1107.5050 [hep-ph]].
 - [3] A. Kurkela and G. D. Moore, *JHEP* **1111** (2011) 120 [arXiv:1108.4684 [hep-ph]].
 - [4] A. Kurkela and E. Lu, arXiv:1405.6318 [hep-ph].
 - [5] S. S. Gubser, D. R. Gulotta, S. S. Pufu and F. D. Rocha, *JHEP* **0810** (2008) 052 [arXiv:0803.1470 [hep-th]].
 - [6] Y. Hatta, E. Iancu and A. H. Mueller, *JHEP* **0805** (2008) 037 [arXiv:0803.2481 [hep-th]].
 - [7] P. M. Chesler, K. Jensen, A. Karch and L. G. Yaffe, *Phys. Rev. D* **79** (2009) 125015 [arXiv:0810.1985 [hep-th]].
 - [8] P. M. Chesler and L. G. Yaffe, *Phys. Rev. Lett.* **106** (2011) 021601 [arXiv:1011.3562 [hep-th]].
 - [9] S. Chatrchyan *et al.* [CMS Collaboration], *Phys. Rev. C* **84** (2011) 024906 [arXiv:1102.1957 [nucl-ex]].
 - [10] S. Chatrchyan *et al.* [CMS Collaboration], *JHEP* **1210** (2012) 087 [arXiv:1205.5872 [nucl-ex]].
 - [11] S. Chatrchyan *et al.* [CMS Collaboration], *Phys. Lett. B* **730** (2014) 243 [arXiv:1310.0878 [nucl-ex]].
 - [12] S. Chatrchyan *et al.* [CMS Collaboration], arXiv:1406.0932 [nucl-ex].
 - [13] G. Aad *et al.* [ATLAS Collaboration], *Phys. Rev. Lett.* **105** (2010) 252303 [arXiv:1011.6182 [hep-ex]].
 - [14] G. Aad *et al.* [ATLAS Collaboration], *Phys. Lett. B* **719** (2013) 220 [arXiv:1208.1967 [hep-ex]].
 - [15] G. Aad *et al.* [ATLAS Collaboration], arXiv:1406.2979 [hep-ex].
 - [16] B. Abelev *et al.* [ALICE Collaboration], *JHEP* **1403** (2014) 013 [arXiv:1311.0633 [nucl-ex]].
 - [17] J. Casalderrey-Solana, D. C. Gulhan, J. G. Milhano, D. Pablos and K. Rajagopal, arXiv:1405.3864 [hep-ph].
 - [18] K. C. Zapp, F. Krauss and U. A. Wiedemann, *JHEP* **1303** (2013) 080 [arXiv:1212.1599 [hep-ph]].
 - [19] R. Baier, Y. L. Dokshitzer, A. H. Mueller, S. Peigne and D. Schiff, *Nucl. Phys. B* **483** (1997) 291 [hep-ph/9607355]; *Nucl. Phys. B* **484** (1997) 265 [hep-ph/9608322];
 - [20] B. G. Zakharov, *JETP Lett.* **63** (1996) 952 [hep-ph/9607440].
 - [21] U. A. Wiedemann, *Nucl. Phys. B* **588** (2000) 303 [hep-ph/0005129].
 - [22] M. Gyulassy, P. Levai and I. Vitev, *Nucl. Phys. B* **594** (2001) 371 [nucl-th/0006010].
 - [23] X. -N. Wang and X. -f. Guo, *Nucl. Phys. A* **696** (2001) 788 [hep-ph/0102230].
 - [24] P. B. Arnold, G. D. Moore and L. G. Yaffe, *JHEP* **0206** (2002) 030 [hep-ph/0204343].
 - [25] P. B. Arnold, S. Cantrell and W. Xiao, *Phys. Rev. D* **81** (2010) 045017 [arXiv:0912.3862 [hep-ph]].
 - [26] S. Caron-Huot, *Phys. Rev. D* **79** (2009) 065039 [arXiv:0811.1603 [hep-ph]].
 - [27] J. Casalderrey-Solana and E. Iancu, *JHEP* **1108** (2011) 015 [arXiv:1105.1760 [hep-ph]].
 - [28] Y. Mehtar-Tani, C. A. Salgado and K. Tywoniuk, *JHEP* **1204** (2012) 064 [arXiv:1112.5031 [hep-ph]].
 - [29] A. Beraudo, J. G. Milhano and U. A. Wiedemann, *JHEP* **1207** (2012) 144 [arXiv:1204.4342 [hep-ph]].
 - [30] J. Casalderrey-Solana, Y. Mehtar-Tani, C. A. Salgado and K. Tywoniuk, *Phys. Lett. B* **725** (2013) 357 [arXiv:1210.7765 [hep-ph]].
 - [31] J. -P. Blaizot, E. Iancu and Y. Mehtar-Tani, *Phys. Rev. Lett.* **111** (2013) 052001 [arXiv:1301.6102 [hep-ph]].
 - [32] J. -P. Blaizot, F. Dominguez, E. Iancu and Y. Mehtar-Tani, *JHEP* **1406** (2014) 075 [arXiv:1311.5823 [hep-ph]].
 - [33] M. Panero, K. Rummukainen and A. Schfer, *Phys. Rev. Lett.* **112** (2014) 162001 [arXiv:1307.5850 [hep-ph]].
 - [34] M. D'Onofrio, A. Kurkela and G. D. Moore, *JHEP* **1403** (2014) 125 [arXiv:1401.7951 [hep-lat]].

- [35] B. Schenke, C. Gale and S. Jeon, Phys. Rev. C **80** (2009) 054913 [arXiv:0909.2037 [hep-ph]].
- [36] N. Armesto, L. Cunqueiro and C. A. Salgado, Eur. Phys. J. C **63** (2009) 679 [arXiv:0907.1014 [hep-ph]].
- [37] K. C. Zapp, Eur. Phys. J. C **74** (2014) 2762 [arXiv:1311.0048 [hep-ph]].
- [38] P. B. Arnold and C. Dogan, Phys. Rev. D **78** (2008) 065008 [arXiv:0804.3359 [hep-ph]].
- [39] E. Braaten and R. D. Pisarski, Nucl. Phys. B **337** (1990) 569;
- [40] P. Aurenche, F. Gelis and H. Zaraket, JHEP **0205** (2002) 043 [hep-ph/0204146].
- [41] P. B. Arnold and W. Xiao, Phys. Rev. D **78** (2008) 125008 [arXiv:0810.1026 [hep-ph]].
- [42] G. Molière, *Z. Naturforsch.* **2 a** (1947) 133, **3 a** (1948) 78, **10 a** (1955) 177.
- [43] F. D'Eramo, M. Lekaveckas, H. Liu and K. Rajagopal, JHEP **1305** (2013) 031 [arXiv:1211.1922 [hep-ph]].
- [44] R. Baier, Y. L. Dokshitzer, A. H. Mueller and D. Schiff, JHEP **0109** (2001) 033 [hep-ph/0106347].